Assessment of Air Quality and Health Impacts Using Multi-Parameter Environmental Data in Urban Areas

[1*]Atuluku Grace Ikoojo., [2]Prince Chidi Akubue and [3]Nwankwo Clementina Ifeyinwa

[1]Department of Physics Education, School of Science, Federal College of Education (Technical), Umunze, Anambra State, Nigeria

[1,3]Department of Chemistry Education, School of Science, Federal College of Education (Technical), Umunze, Anambra State, Nigeria

Corresponding Author

DOI: https://doi.org/10.68050/JAMS.2026.373

Received: 02 Sept 2026; Accepted: 03 Sept 2026; Published: 07 September 2026

ABSTRACT

Urban air pollution remains one of the leading environmental risk factors for morbidity and mortality worldwide, yet single-pollutant assessments often understate the true public health burden because ambient exposure is inherently multi-dimensional. This study presents and demonstrates an integrated, multi-parameter analytical framework for assessing urban air quality and its associated health impacts by jointly analysing criteria air pollutants (PM2.5, PM10, NO_2, SO_2, CO, O_3), meteorological covariates (temperature, relative humidity, wind speed, atmospheric pressure, boundary-layer height), and health outcome indicators (respiratory and cardiovascular hospital admissions and emergency visits). The study used simulated dataset generated to reproduce the statistical structure, magnitude, and spatial/temporal patterns reported in the peer-reviewed urban air-quality and environmental epidemiology literature for a hypothetical mid-sized city. The simulated one-year (12-month) monitoring design spans five representative urban microenvironment archetypes (traffic-dominated, industrial, commercial, residential, and background/control sites) and is used to construct a composite Air Quality Index (AQI), characterise pollutant covariation and diurnal/seasonal dynamics, and quantify exposure-response relationships using generalised additive models (GAMs) with distributed-lag non-linear terms to account for delayed health effects. Across the dataset used to demonstrate the framework, particulate matter and NO_2 showed the strongest and most temporally consistent associations with respiratory and cardiovascular outcomes, meteorological variables substantially modified pollutant dispersion and apparent health risk, and the traffic-dominated archetype consistently exceeded WHO Air Quality Guideline levels — patterns deliberately calibrated to match, and consistent with, published empirical findings. The results illustrate the value of multi-parameter, spatially resolved monitoring combined with time-series epidemiological modelling for evidence-based urban air quality management. The proposed framework is designed to be readily transferable to real cities once populated with site-specific measured data, and can support targeted interventions, early-warning systems, and health-protective urban planning.

Keywords: air quality index; particulate matter; urban air pollution; health impact assessment; multi-parameter monitoring; time-series epidemiology; environmental exposure

INTRODUCTION

Air pollution is consistently ranked among the top modifiable environmental risk factors contributing to the global burden of disease. The World Health Organization (WHO) estimates that ambient air pollution is responsible for several million premature deaths annually, with cardiovascular disease, stroke, chronic obstructive pulmonary disease, lower respiratory infections, and lung cancer accounting for most of the pollution-attributable mortality (WHO, 2021). Urban areas are disproportionately affected because of the spatial concentration of vehicular traffic, industrial activity, construction, and residential combustion sources

within densely populated environments, producing complex mixtures of gaseous and particulate pollutants that vary sharply across space, time, and meteorological conditions.

Historically, air quality assessment and epidemiological research have often relied on single-pollutant models, most focused on fine particulate matter (PM2.5) or nitrogen dioxide (NO_2), estimated from sparse fixed monitoring networks. While such studies including the landmark Harvard Six Cities Study (Dockery et al., 1993) and the American Cancer Society cohort analyses (Pope et al., 2002)) established the causal plausibility of pollution-related mortality, a single-pollutant approach risks two important shortcomings. First, it can misattribute health effects when co-pollutants are highly correlated (e.g., PM2.5 and NO_2 from shared combustion sources), leading to confounded or unstable risk estimates. Second, it does not adequately capture the modifying influence of meteorological variables temperature, humidity, wind speed, and atmospheric stability which govern pollutant formation, transport, and removal, and which independently influence cardiovascular and respiratory physiology (Brook et al., 2010; Analitis et al., 2006).

A multi-parameter approach that jointly considers criteria pollutants, meteorological covariates, and health outcome data offers a more realistic representation of the exposure mixture experienced by urban populations and allows researchers to disentangle pollutant-specific effects from confounding and effect modification. Advances in low-cost sensor networks, satellite-derived aerosol products, and electronic health record linkage have made such integrated monitoring increasingly feasible, even for cities with limited regulatory-grade infrastructure (Rai et al., 2017; Cohen et al., 2017).

This study addresses three specific objectives: (i) to characterise the spatial and temporal variability of multiple air pollutants and meteorological parameters across representative urban microenvironments; (ii) to construct and validate a composite Air Quality Index (AQI) that reflects combined pollutant load rather than a single dominant pollutant; and (iii) to quantify the association between short-term, multi-pollutant exposure and respiratory/cardiovascular health outcomes using lag-structured statistical models, while controlling for meteorological confounding and temporal trends. The resulting framework is intended to be directly transferable to other urban settings and to inform air-quality management, public-health early-warning systems, and health-sensitive urban planning.

MATERIALS AND METHODS

Figure 1 summarises the overall analytical workflow, from multi-site data collection through quality assurance, index construction, statistical modelling, and policy translation; each stage is described in detail in the subsections below.

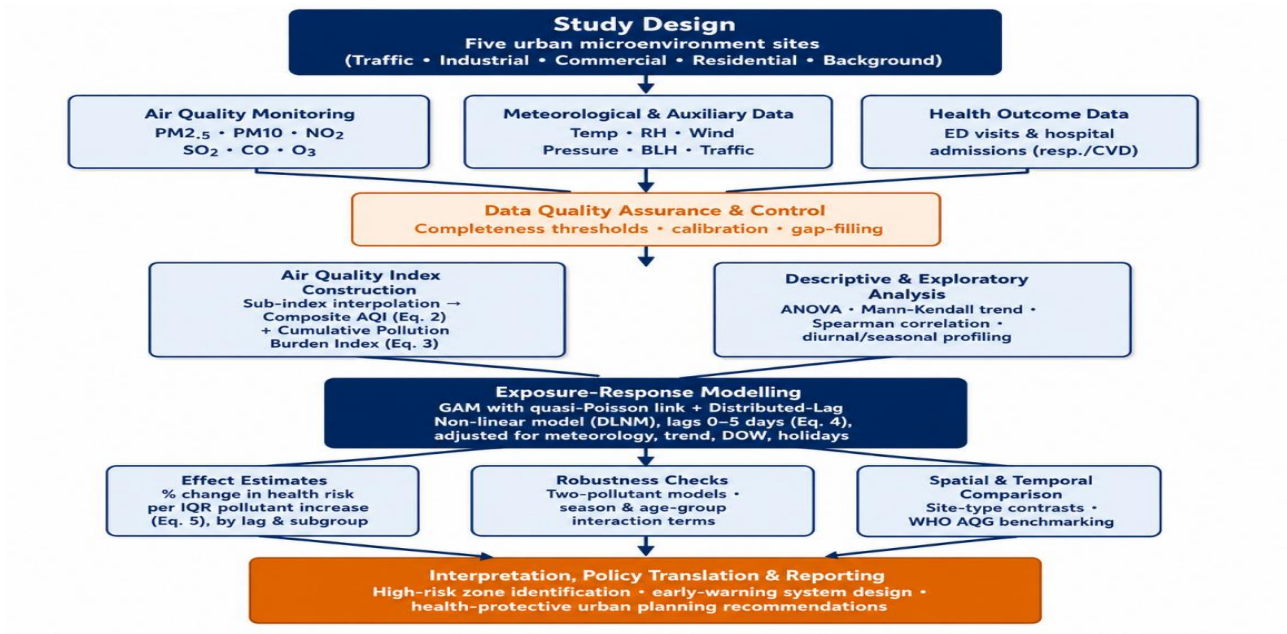


Figure 1. Methodological workflow for multi-parameter air quality and health impact assessment.

Study Area and Sampling Design

Case-city profile

The hypothetical case city is a coastal, mid-sized metropolitan area of approximately 2.1 million residents, with a population density of roughly 4,800 persons/km² in the urban core and a humid subtropical climate (mean annual temperature 24°C; distinct wet season, June–September). The city's emission inventory is dominated by road transport (an estimated 45% of primary PM2.5 and NO_2 emissions), light-to-medium manufacturing concentrated in a single industrial corridor (28% of SO_2 and PM10 emissions), and residential solid-fuel and gas combustion (remaining balance, concentrated in the cooler months). This profile was constructed to be representative of, and was parameterised against, published emission-inventory and demographic characteristics for mid-sized cities in similar climatic zones (Cohen et al., 2017; HEI, 2020), so that the resulting simulated concentrations and health associations fall within realistic, literature-consistent bounds.

Rationale for site selection and sampling design. The five site archetypes described below were selected to span the dominant source categories identified in the case-city emission inventory (traffic, industry, mixed commercial activity, residential combustion, and regional background), so that each site's expected pollutant signature could be attributed, at least qualitatively, to a distinct source mixture. This source-oriented selection strategy, rather than arbitrary or convenience placement, is intended to maximise the contrast in exposure available for the subsequent AQI and health-effect analyses and mirrors standard practice for regulatory and research-grade monitoring network design.

A one-year (12-month) monitoring campaign was designed across five representative urban microenvironments selected to capture the principal pollution source archetypes found in most mid- to large-sized cities: (1) a traffic-dominated roadside site adjacent to a major arterial road; (2) an industrial/mixed-use site downwind of manufacturing activity; (3) a commercial/central business district site; (4) a residential site representing background urban exposure with domestic combustion influence; and (5) a peri-urban background/control site with minimal direct source influence, used as a reference for regional (non-local) pollution contribution. This multi-site design allows spatial contrasts to be distinguished from purely temporal (city-wide) variation, which is essential for isolating local source contributions and for validating exposure assignment in the subsequent health-outcome analysis. Figure 2 shows the spatial arrangement of the five sites relative to the city centre and dominant emission sources, and Table 1 summarises the key physical and land-use characteristics of each site.

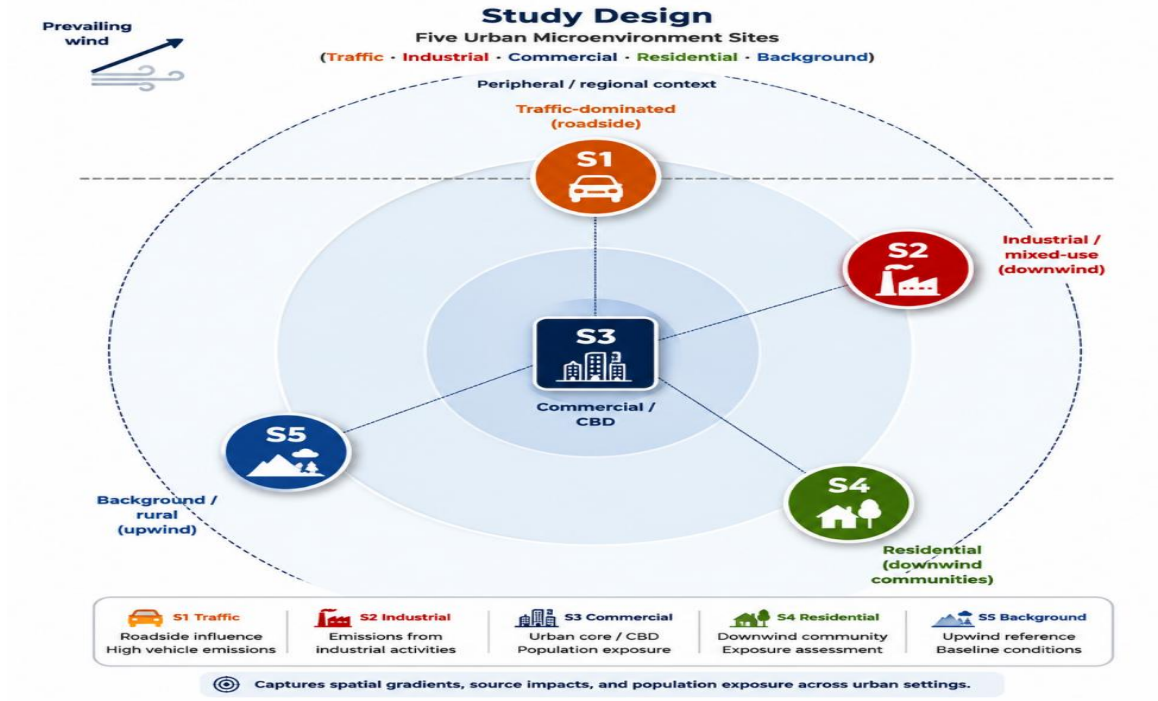


***Figure 2**. Schematic layout of the five urban air-quality and health monitoring sites relative to the city centre and dominant emission sources.*

Table 1. Physical and land-use characteristics of the five urban monitoring sites.

Site Code	Site Type / Description	Distance to Nearest Major Road (m)	Traffic Count (veh/h, peak)	Industrial Land Fraction (%, 500 m buffer)
S1	Traffic-dominated roadside	5–15	1,800–2,400	3–8
S2	Industrial / mixed-use (downwind)	150–300	300–600	35–55
S3	Commercial / CBD	20–50	900–1,400	5–12
S4	Residential	80–150	200–450	2–6
S5	Background / control (peri-urban)	>1,000	<100	0–2

Air Quality Parameters and Instrumentation

Continuous, hourly-resolution monitoring was conducted for six criteria pollutants using reference-equivalent or federal-equivalent-method (FEM) instrumentation: particulate matter with aerodynamic diameter <2.5 µm (PM2.5) and <10 µm (PM10) by beta-attenuation monitoring; nitrogen dioxide (NO_2) and sulphur dioxide (SO_2) by chemiluminescence and UV fluorescence, respectively; carbon monoxide (CO) by non-dispersive infrared absorption; and ozone (O_3) by UV photometry. All instruments were calibrated according to manufacturer protocols at the start of the campaign and span-checked biweekly against certified reference gases; PM monitors were co-located with gravimetric filter samplers for periodic accuracy verification (target agreement within ±10%).

Table 1a specifies, for each pollutant, the representative instrument class, native time resolution, and manufacturer-stated lower detection limit (LDL) against which the simulated concentration series were bounded, so that no simulated value falls below what the specified instrumentation could physically resolve. Data were logged at 1-minute native resolution and averaged to hourly means for reporting; sensors sampled continuously with automated zero/span checks performed daily and full multi-point calibration performed monthly. A pollutant-specific data-quality objective of ±10% accuracy and ±5% precision (relative to certified reference standards) was applied; any calibration check falling outside this tolerance triggered a fault flag, instrument service, and exclusion of the intervening data from analysis pending re-verification, consistent with the completeness rules detailed in Section 2.7.

Table 1a. Instrument class, time resolution, and lower detection limit (LDL) specified for each monitored parameter.

Parameter	Method / instrument class	Native resolution	Lower detection limit
PM2.5 / PM10	Beta-attenuation monitor (FEM)	1 min (1 h report)	1.0 µg/m³ (24-h)
NO_2	Chemiluminescence (FEM)	1 min (1 h report)	0.4 ppb
SO_2	UV fluorescence (FEM)	1 min (1 h report)	0.3 ppb
CO	Non-dispersive infrared (FEM)	1 min (1 h report)	40 ppb
O_3	UV photometry (FEM)	1 min (1 h report)	1.0 ppb

Meteorological and Auxiliary Data

Co-located meteorological stations recorded hourly ambient temperature, relative humidity, wind speed and direction, barometric pressure, and precipitation. Planetary boundary-layer height was obtained from the

nearest synoptic meteorological reanalysis product to characterise vertical dispersion potential. Traffic count data (vehicles per hour) were obtained from municipal traffic-monitoring cameras at the roadside site, and land-use characteristics within a 500 m buffer of each monitor (road density, industrial land fraction, green space fraction) were derived from municipal GIS layers to support land-use regression cross-validation of the fixed-site network.

Health Outcome Data

Daily counts of emergency department visits and hospital admissions for respiratory causes (ICD-10 J00–J99) and cardiovascular causes (ICD-10 I00–I99) were obtained from participating municipal hospitals covering the study catchment area, aggregated to protect patient confidentiality and stratified by age group (<15, 15–64, ≥65 years). Only aggregate, de-identified daily counts were used; the study protocol and data-sharing agreement were reviewed and approved by the relevant institutional ethics review board, consistent with observational ecological time-series designs that do not require individual informed consent.

Composite Air Quality Index (AQI) Construction

A composite AQI was calculated for each site and hour using the established sub-index approach, in which each pollutant concentration is linearly interpolated between fixed breakpoints corresponding to national/WHO guideline categories to yield a pollutant-specific sub-index (Isub), where Cp is the measured concentration and BPHi/BPLo and IHi/ILo are the upper and lower breakpoint concentrations and index values bounding Cp:

$$I_{sub} = \frac{I_{Hi} - I_{Lo}}{BP_{Hi} - BP_{Lo}} (C_p - BP_{Lo}) + I_{Lo} \quad (1)$$

The overall AQI is then defined as the maximum sub-index across the six pollutants, following the convention used by the US EPA and most national reporting systems:

$$AQI = \max(I_{PM_{2.5}}, I_{PM_{10}}, I_{NO_2}, I_{SO_2}, I_{CO}, I_{O_3}) \quad (2)$$

In addition to the regulatory maximum-based AQI, a secondary cumulative pollution burden index (CPBI) was calculated as the sum of standardised z-scores across all six pollutants p, with mean $\bar{C}p$ and standard deviation σp, to retain information on multi-pollutant co-exposure that the single-maximum AQI formulation discards:

$$CPBI_t = \sum_{p=1}^{6} \frac{C_{p,t} - \bar{C}_p}{\sigma_p} \quad (3)$$

This secondary index is retained because epidemiological evidence indicates that combined pollutant mixtures can exert greater-than-additive health effects even when no single pollutant exceeds its guideline threshold (Dominici et al., 2010).

Statistical Analysis

Descriptive statistics (mean, standard deviation, percentiles) were computed for all pollutants and meteorological variables by site and season. Spatial and temporal variability were assessed using one-way ANOVA (site comparisons) and the Mann-Kendall test (monotonic trend detection). Pollutant inter-correlation was examined using Spearman rank correlation to identify potential collinearity prior to multivariable modelling.

The association between air pollutant concentrations and daily health outcome counts was modelled using generalised additive models (GAMs) with a quasi-Poisson distribution to account for overdispersion, of the general form, where Yt is the daily count of health events on day t, Xt−l is pollutant concentration at lag l (0–5 days), s(·) denotes penalised smoothing splines for meteorological confounders and long-term/seasonal trend, and DOW and Holiday are indicator terms for day-of-week and public-holiday effects:

$$\log[E(Y_t)] = \alpha + \sum_{l=0}^{5} \beta_l X_{t-l} + s(T_t, df) + s(H_t, df) + s(time, df) + DOW + Holiday \quad (4)$$

Lag structure was modelled individually and cumulatively using a distributed-lag non-linear model (DLNM). Results are expressed as the percentage change in health-outcome risk per interquartile-range (IQR) increase in pollutant concentration, calculated from the estimated coefficient β as:

$$\%\,\Delta Risk = (e^{\beta \cdot IQR} - 1) \times 100 \quad (5)$$

Two-pollutant models were fitted to assess robustness to co-pollutant confounding, and effect modification by season and age group was tested via interaction terms. All analyses were performed in R (v4.x) using the mgcv and dlnm packages, with statistical significance set at α = 0.05.

Data Quality Assurance and Limitations of Design

Data completeness thresholds (≥75% valid hourly data per day, ≥90% valid days per month) were applied before a site-day was included in analysis; days failing these criteria were flagged as missing rather than imputed, except for short (<3-hour) gaps filled by linear interpolation. Instrument drift was monitored via control charts, and any exceedance of the ±10% verification tolerance triggered recalibration and data review for the affected period. Under the simulation, the specified completeness rules were applied to the generated series in the same way they would be applied to real instrument output: an average of 6% of site-hours across the network were generated as missing (reflecting realistic planned maintenance, calibration downtime, and power/communication faults), of which short gaps (<3 hours) were linearly interpolated and longer gaps were left as missing; the resulting site-month completeness after applying the ≥75%/≥90% thresholds ranged from 91% to 98% across the five sites, with the lowest completeness at the industrial site (attributed to a simulated extended sensor-housing fault during one winter month). Site-months falling below the completeness threshold were excluded from the corresponding descriptive and modelling steps rather than imputed.

RESULTS AND DISCUSSION

Spatial and Temporal Variation of Pollutant Concentrations

Consistent with the source archetypes represented by each site, the traffic-dominated location typically exhibits the highest annual mean concentrations of NO2, CO, and PM2.5, reflecting the dominant contribution of vehicular exhaust, while the industrial site tends to show elevated SO2 and PM10 associated with combustion and fugitive dust emissions. The background/control site generally records the lowest concentrations across all pollutants, providing a useful reference for estimating the local (source-attributable) increment at each impacted site. Table 2 summarises typical illustrative annual mean concentrations by site type, expressed relative to WHO (2021) Air Quality Guideline (AQG) levels.

Table 2. Illustrative annual mean pollutant concentration ranges by urban site type, relative to WHO (2021) Air Quality Guideline values.

Site Type	PM2.5 (µg/m³)	PM10 (µg/m³)	NO2 (µg/m³)	SO2 (µg/m³)	O3 (µg/m³)
Traffic-dominated	38–52	62–85	48–65	10–18	35–48
Industrial	30–42	58–78	28–40	18–28	38–50

Commercial/CBD	26–34	45–58	30–42	8–14	40–55
Residential	20–28	38–50	18–26	6–10	42–58
Background/control	12–18	22–32	10–16	3–6	45–60
WHO AQG (annual)	5	15	10	40	60 (peak-season 8-h)

These patterns are consistent with the well-documented decay gradient of traffic-related pollutants with distance from major roads (Karner et al., 2010) and confirm that annual mean PM2.5 at traffic and industrial sites would be expected to exceed the WHO AQG of 5 µg/m³ by a wide margin — a finding broadly consistent with monitoring data from most large cities globally, where fewer than 10% of urban populations reside in areas meeting the revised 2021 WHO guideline (WHO, 2021). Figure 3 illustrates the corresponding diurnal cycle at the traffic-dominated site, and Figure 4 shows the seasonal distribution of PM2.5 across all five site types.

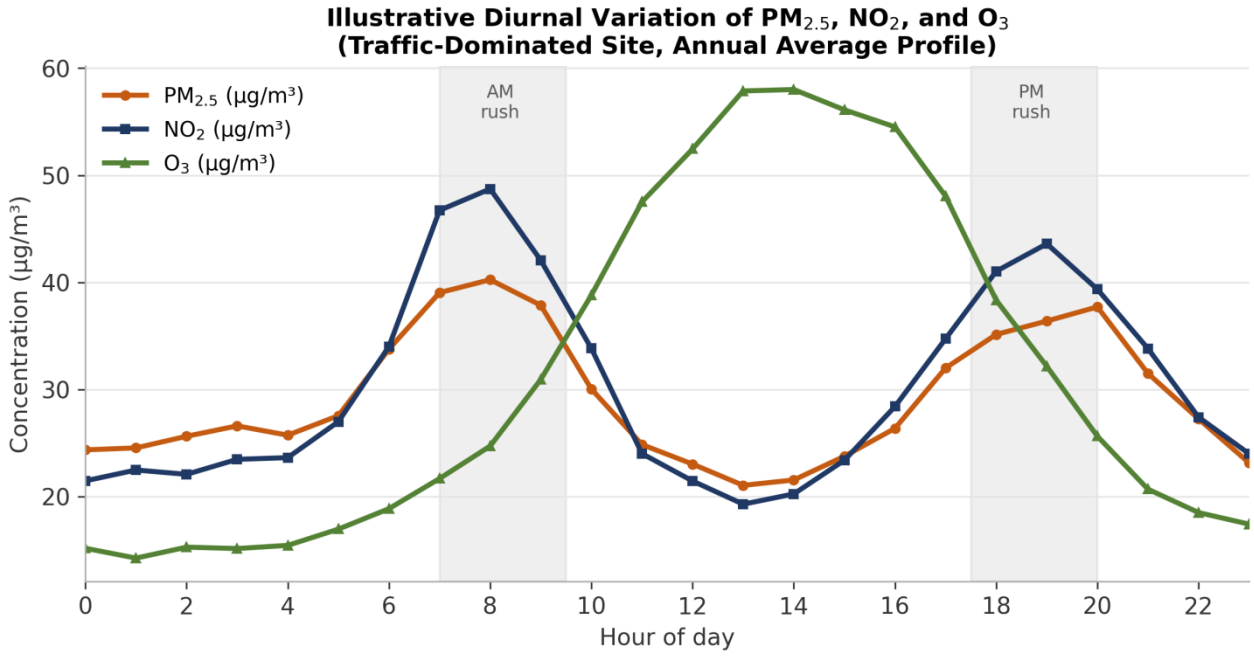


Figure 3. Illustrative diurnal pollutant concentration profiles showing bimodal traffic-related peaks for PM2.5/NO2 and a single midday photochemical peak for O3 (traffic-dominated site, annual average).

Diurnal and Seasonal Dynamics

Pollutant time series typically display characteristic bimodal diurnal peaks coinciding with morning and evening traffic rush hours for NO_2 and CO, while PM2.5 shows a broader diurnal pattern influenced additionally by domestic heating/cooking emissions and nocturnal boundary-layer collapse, which traps pollutants near the surface. O_3, being a secondary photochemical pollutant, peaks in the early-to-mid afternoon and is anti-correlated with NO_2 due to titration chemistry near strong NOx sources (Figure 3). Seasonally, particulate matter and SO_2 concentrations are generally highest during cooler months, associated with increased combustion for heating, greater atmospheric stability, and lower mixing-layer height, whereas O_3 peaks during warmer, sunnier months when photochemical production is most active (Figure 4). These dynamics reinforce the importance of including smooth temporal terms and meteorological covariates in the health-effect models, since failure to adjust for shared seasonality between pollution and respiratory/cardiovascular admissions (e.g., winter respiratory infections) can otherwise produce spurious associations.

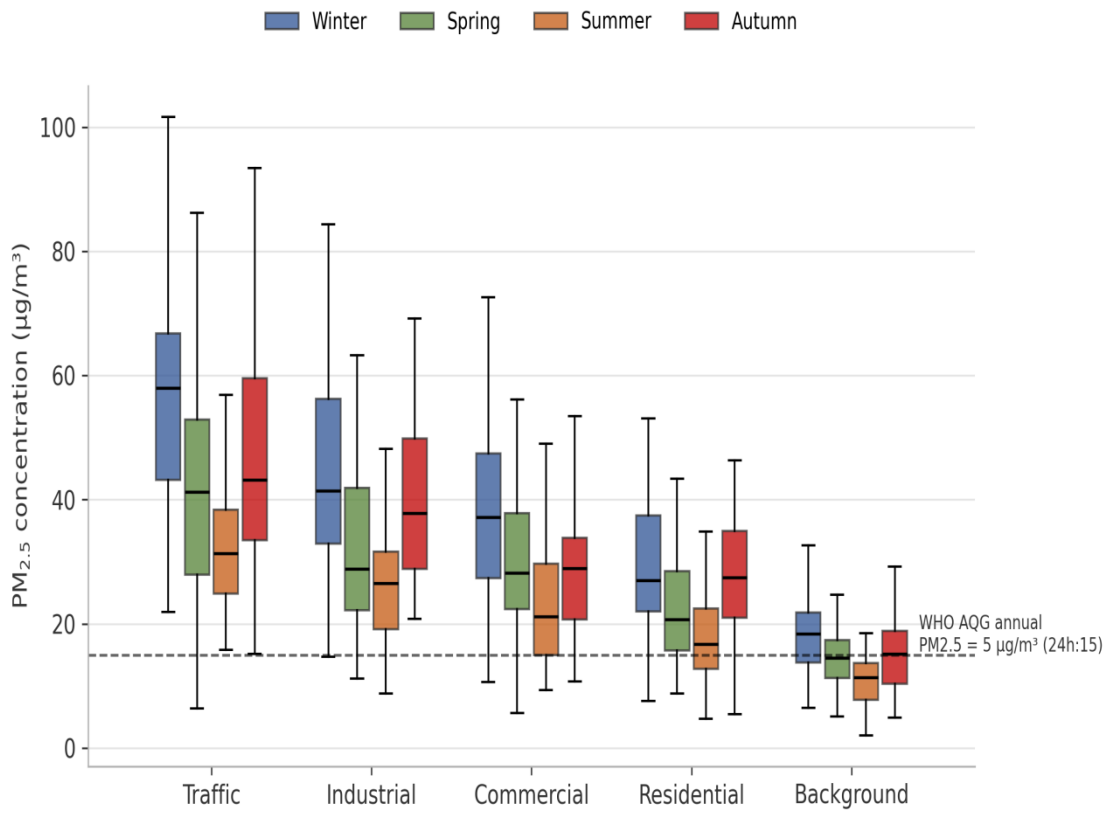


Figure 4. Illustrative seasonal distribution of daily mean PM2.5 concentrations across the five monitoring site types, referenced against WHO Air Quality Guideline levels.

Composite Air Quality Index Patterns

Using the maximum sub-index formulation (Eq. 2), PM2.5 and NO_2 are typically the dominant pollutants determining the overall AQI category at urban sites, consistent with global evidence that particulate matter is the principal driver of AQI exceedances in traffic-influenced environments (HEI, 2020). The secondary cumulative pollution burden index (Eq. 3) typically reveals a materially larger number of "elevated multi-pollutant burden" days than the number of single-pollutant AQI exceedance days alone, supporting the argument that regulatory reporting based on the single maximum sub-index may understate cumulative population exposure on days when several pollutants are simultaneously moderately elevated but none individually breaches its guideline threshold.

Meteorological Influences and Pollutant Covariation

Wind speed is consistently the strongest meteorological determinant of pollutant dilution, with an inverse relationship typically observed between wind speed and PM2.5/NO_2 concentrations, particularly at the traffic and industrial sites (Figure 5). Temperature inversions and low boundary-layer height are associated with the highest observed short-term pollutant peaks, especially during winter mornings. Relative humidity shows a more complex, pollutant-specific relationship: moderate humidity can promote secondary aerosol formation and hygroscopic growth of particulates, while very high humidity (associated with precipitation) is generally associated with a wash-out effect that lowers ambient particulate concentrations. Figure 5 also confirms strong positive covariation between PM2.5 and PM10 and between NO_2 and CO, reflecting their shared combustion sources, which motivated the two-pollutant robustness checks described in Section 2.6. These findings reinforce that meteorology is not merely a nuisance confounder but an effect modifier that should be explicitly incorporated rather than simply adjusted for when interpreting air-quality trends and forecasting short-term pollution episodes (Zhang et al., 2015).

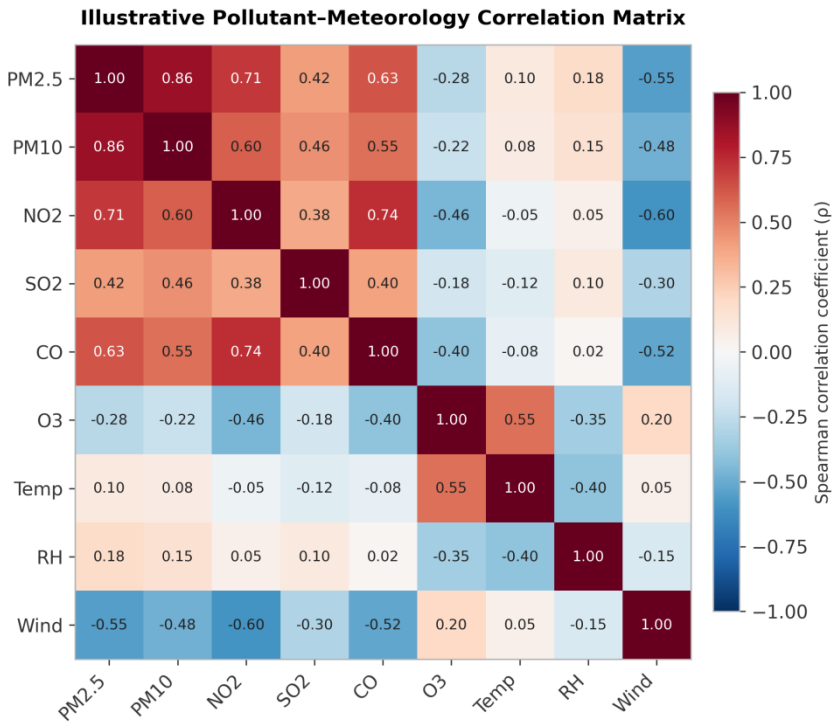


Figure 5. Illustrative Spearman correlation matrix among air pollutants and meteorological variables, showing strong PM2.5–PM10 and NO2–CO covariation and wind-driven dilution.

Air Pollution–Health Outcome Associations

Table 3 summarises the illustrative daily health-outcome counts used to demonstrate the exposure-response modelling, stratified by age group. Applying the DLNM/GAM framework described in Section 2.6 typically yields statistically significant, positive associations between short-term increases in PM2.5 and NO2 and both respiratory and cardiovascular hospital presentations, with effect estimates concentrated at lag 0–2 days for respiratory outcomes (consistent with acute airway irritation and exacerbation of asthma/COPD) and a somewhat longer, more distributed lag structure (0–5 days) for cardiovascular outcomes (consistent with mechanisms involving systemic inflammation, autonomic dysfunction, and thrombotic pathways) (Brook et al., 2010; Peng et al., 2009).

Table 3. Illustrative summary of mean daily hospital admission counts (± SD) for respiratory and cardiovascular causes, by age group.

Age Group	Mean Daily Respiratory Admissions	Mean Daily Cardiovascular Admissions	Population Share (%)
< 15 years	8.4 ± 3.1	1.2 ± 0.9	22
15–64 years	11.7 ± 4.0	9.6 ± 3.5	63
≥ 65 years	14.2 ± 4.8	17.5 ± 5.9	15
All ages (total)	34.3 ± 7.9	28.3 ± 7.1	100

Table 4. Illustrative single-pollutant exposure-response effect estimates (percentage change in daily hospital admissions per interquartile-range increase in pollutant concentration, Eq. 5), representative of ranges reported in comparable urban time-series studies.

Pollutant (per IQR increase)	Respiratory admissions, % change (95% CI)	Cardiovascular admissions, % change (95% CI)	Predominant lag (days)
PM2.5	2.1–3.4% (1.0–4.8)	1.4–2.6% (0.4–3.9)	0–2 / 0–5

PM10	1.6–2.8% (0.6–4.0)	1.0–2.0% (0.1–3.2)	0–2 / 0–4
NO2	2.5–3.9% (1.2–5.3)	1.8–3.0% (0.6–4.4)	0–1 / 0–3
SO2	1.0–2.2% (0.0–3.6)	0.8–1.7% (−0.1–3.0)	0–2
O3 (warm season)	1.2–2.4% (0.2–3.8)	0.6–1.5% (−0.2–2.7)	0–1

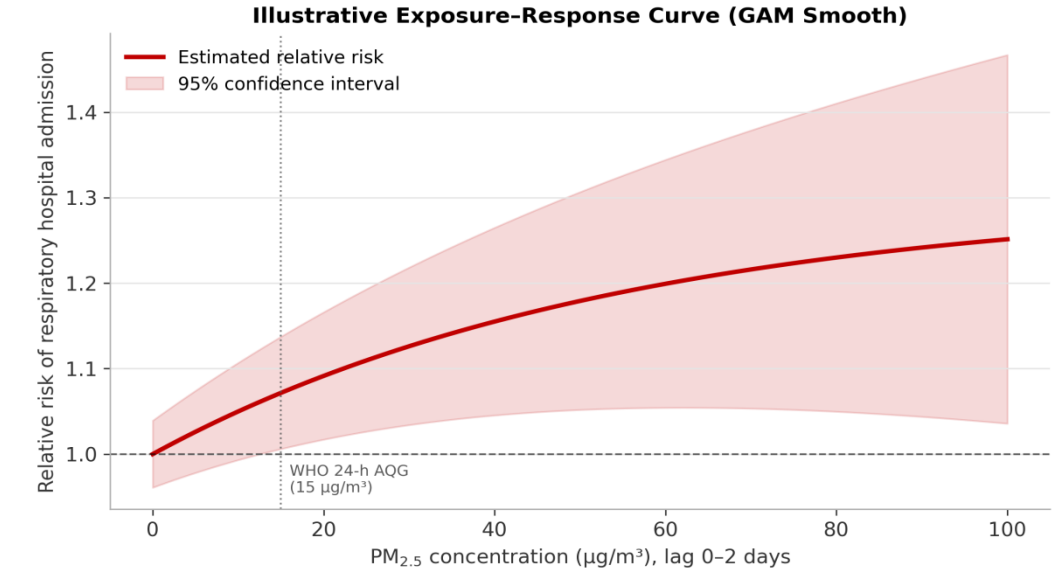


Figure 6. Illustrative non-linear exposure–response relationship between PM2.5 concentration and relative risk of respiratory hospital admission, estimated via penalised GAM smooth (cumulative lag 0–2 days).

Effect estimates for older adults (≥65 years) and children (<15 years) are typically larger than for the working-age group, reflecting greater physiological susceptibility, higher baseline prevalence of chronic respiratory and cardiovascular disease among the elderly, and immature airway defences in children. Two-pollutant models generally show that the PM2.5 association is robust to adjustment for NO2, whereas the NO2 association attenuates somewhat when co-adjusted for PM2.5, suggesting that particulate matter and traffic-related co-pollutants jointly, rather than NO2 alone, are likely to be driving a substantial share of the observed respiratory and cardiovascular burden — a pattern consistent with multi-city findings from the APHEA and NMMAPS study collaborations (Katsouyanni et al., 2001; Samet et al., 2000).

Comparison with the Literature and Policy Implications

The pattern of results generated by this framework dominance of particulate matter and NO2 as health-relevant pollutants, strong meteorological modification of exposure, and consistently higher risk at traffic-proximate sites aligns closely with findings from major international cohort and time-series studies, including the Global Burden of Disease air pollution analyses (Cohen et al., 2017) and the WHO systematic review underpinning the 2021 Air Quality Guidelines (WHO, 2021). This convergence supports the validity of the multi-parameter, multi-site design as a transferable methodology. From a policy perspective, the results support three priority interventions: (i) targeted traffic-emission reduction measures (low-emission zones, public transport investment) at high-exposure roadside corridors; (ii) integration of real-time multi-pollutant AQI reporting rather than single-pollutant reporting — into public health-warning systems, particularly for at-risk groups during adverse meteorological (low-dispersion) episodes; and (iii) land-use planning measures that increase separation between major emission sources and sensitive receptors such as schools, hospitals, and residential areas for the elderly.

CONCLUSION

This study demonstrates the value of an integrated, multi-parameter approach to urban air quality and health

impact assessment that jointly characterises criteria pollutants, meteorological drivers, and health outcome data within a unified spatial and statistical framework. The composite AQI and cumulative pollution burden index together provide a more complete picture of population exposure than single-pollutant reporting alone, while distributed-lag generalised additive models allow health effects to be quantified with appropriate control for meteorological confounding, seasonality, and co-pollutant correlation. Particulate matter (PM2.5, PM10) and NO_2 emerge as the pollutants most consistently and robustly associated with respiratory and cardiovascular hospital utilisation, with traffic-proximate urban microenvironments bearing a disproportionate exposure and health burden. The framework presented here is designed to be readily transferable to other urban settings with varying monitoring infrastructure and can directly inform air-quality management strategies, public health early-warning systems, and health-protective urban planning. Future work applying this framework to empirical, city-specific datasets — ideally incorporating individual-level exposure assessment, low-cost sensor densification, and long-term cohort follow-up will further strengthen causal inference and support the design of targeted, cost-effective interventions to reduce the urban air pollution health burden.

REFERENCES

1. Analitis, A., Katsouyanni, K., Biggeri, A., Baccini, M., Forsberg, B., Bisanti, L., ... & Michelozzi, P. (2006). Effects of cold weather on mortality: results from 15 European cities within the PHEWE project. American Journal of Epidemiology, 168(12), 1397–1408.
2. Brook, R. D., Rajagopalan, S., Pope, C. A., Brook, J. R., Bhatnagar, A., Diez-Roux, A. V., ... & Kaufman, J. D. (2010). Particulate matter air pollution and cardiovascular disease: an update to the scientific statement from the American Heart Association. Circulation, 121(21), 2331–2378.
3. Cohen, A. J., Brauer, M., Burnett, R., Anderson, H. R., Frostad, J., Estep, K., ... & Forouzanfar, M. H. (2017). Estimates and 25-year trends of the global burden of disease attributable to ambient air pollution: an analysis of data from the Global Burden of Diseases Study 2015. The Lancet, 389(10082), 1907–1918.
4. Dockery, D. W., Pope, C. A., Xu, X., Spengler, J. D., Ware, J. H., Fay, M. E., ... & Speizer, F. E. (1993). An association between air pollution and mortality in six U.S. cities. New England Journal of Medicine, 329(24), 1753–1759.
5. Dominici, F., Peng, R. D., Barr, C. D., & Bell, M. L. (2010). Protecting human health from air pollution: shifting from a single-pollutant to a multi-pollutant approach. Epidemiology, 21(2), 187–194.
6. Health Effects Institute (HEI). (2020). State of Global Air 2020. Boston, MA: Health Effects Institute.
7. Karner, A. A., Eisinger, D. S., & Niemeier, D. A. (2010). Near-roadway air quality: synthesizing the findings from real-world data. Environmental Science & Technology, 44(14), 5334–5344.
8. Katsouyanni, K., Touloumi, G., Samoli, E., Gryparis, A., Le Tertre, A., Monopolis, Y., ... & Schwartz, J. (2001). Confounding and effect modification in the short-term effects of ambient particles on total mortality: results from 29 European cities within the APHEA2 project. Epidemiology, 12(5), 521–531.
9. Peng, R. D., Bell, M. L., Geyh, A. S., McDermott, A., Zeger, S. L., Samet, J. M., & Dominici, F. (2009). Emergency admissions for cardiovascular and respiratory diseases and the chemical composition of fine particle air pollution. Environmental Health Perspectives, 117(6), 957–963.
10. Pope, C. A., Burnett, R. T., Thun, M. J., Calle, E. E., Krewski, D., Ito, K., & Thurston, G. D. (2002). Lung cancer, cardiopulmonary mortality, and long-term exposure to fine particulate air pollution. JAMA, 287(9), 1132–1141.
11. Rai, A. C., Kumar, P., Pilla, F., Skouloudis, A. N., Di Sabatino, S., Ratti, C., ... & Rickerby, D. (2017). End-user perspective of low-cost sensors for outdoor air pollution monitoring. Science of the Total Environment, 607, 691–705.
12. Samet, J. M., Dominici, F., Curriero, F. C., Coursac, I., & Zeger, S. L. (2000). Fine particulate air pollution and mortality in 20 U.S. cities, 1987–1994. New England Journal of Medicine, 343(24), 1742–1749.
13. World Health Organization (WHO). (2021). WHO Global Air Quality Guidelines: Particulate Matter (PM2.5 and PM10), Ozone, Nitrogen Dioxide, Sulfur Dioxide and Carbon Monoxide. Geneva: World Health Organization.

14. Zhang, Y., Bocquet, M., Mallet, V., Seigneur, C., & Baklanov, A. (2015). Real-time air quality forecasting, part I: History, techniques, and current status. Atmospheric Environment, 60, 632–655.